SUPPLEMENT TO "STATISTICAL ESTIMATION OF THE STRUCTURAL SIMILARITY INDEX FOR IMAGE QUALITY ASSESSMENT"

FELIPE OSORIO, RONNY VALLEJOS, WILSON BARRAZA, SILVIA OJEDA, AND MARCOS A. LANDI

SUMMARY. In this supplement some additional simulation results are presented. An explicit expression for the expected information matrix is derived and provide some details about the computational implementation of the gradient statistic for the nonlinear regression model with multiplicative noise described at Section 2 from the manuscript. A brief description of the filters used in the work as well as additional results of the simulation study are also presented.

APPENDIX A. ADDITIONAL SIMULATION RESULTS

Tables 1 and 2 present the averages of parameter estimates for the SSIM index for Lena and Baboon reference images. The results were obtained from 1,000 Monte Carlo simulations.

TABLE 1. Averages of parameter estimates of the SSIM index for Lena image.

Number of looks	No filter			Lee filter		
	$\widehat{\alpha}$	$\widehat{\beta}$	$\widehat{\gamma}$	$\widehat{\alpha}$	$\widehat{\beta}$	$\widehat{\gamma}$
1	1.000	1.000	1.000	1.001	1.001	1.020
2	1.000	1.000	1.002	1.007	1.008	1.117
4	1.004	1.004	1.084	1.061	1.068	1.420
8	1.054	1.062	1.404	1.183	1.201	1.875
16	1.182	1.205	1.759	1.306	1.341	2.410
32	1.388	1.436	2.381	0.762	0.811	2.574
Number of looks	Enhanced Lee filter			Kuan filter		
	$\widehat{\alpha}$	$\widehat{\beta}$	$\widehat{\gamma}$	$\widehat{\alpha}$	$\widehat{\beta}$	$\widehat{\gamma}$
1	1.001	1.001	1.029	1.003	1.003	1.064
2	1.018	1.019	1.203	1.022	1.024	1.218
4	1.098	1.106	1.603	1.098	1.106	1.607
8	1.191	1.223	2.388	1.235	1.260	2.300
16	1.000	1.000	1.000	1.011	1.007	1.014
32	1.000	1.000	1.000	1.000	1.000	1.000

The main manuscript has not undergone improvements or corrections. The Version of record of the article is published in *Signal, Image and Video Processing*, and is available online at https://doi.org/10.1007/s11760-021-02051-9.

Table 2. Averages of parameter estimates of the SSIM index for Baboon image.

Number of looks	No filter $\widehat{\alpha}$	No filter $\widehat{\beta}$	No filter $\widehat{\gamma}$	Lee filter $\widehat{\alpha}$	Lee filter $\widehat{\beta}$	Lee filter $\widehat{\gamma}$
1	1.000	1.000	1.003	1.001	1.001	1.050
2	1.001	1.001	1.038	1.010	1.010	1.166
4	1.014	1.015	1.189	1.052	1.054	1.422
8	1.096	1.104	1.579	1.093	1.097	1.692
16	1.238	1.259	2.161	1.008	1.012	1.739
32	1.094	1.144	2.784	0.711	0.715	1.652
Number of looks	**Enhanced Lee filter $\widehat{\alpha}$**	**Enhanced Lee filter $\widehat{\beta}$**	**Enhanced Lee filter $\widehat{\gamma}$**	**Kuan filter $\widehat{\alpha}$**	**Kuan filter $\widehat{\beta}$**	**Kuan filter $\widehat{\gamma}$**
1	1.001	1.001	1.054	1.003	1.003	1.076
2	1.019	1.019	1.219	1.023	1.023	1.243
4	1.067	1.068	1.517	1.107	1.109	1.642
8	1.092	1.095	1.902	1.124	1.129	2.146
16	0.711	0.715	1.809	0.660	0.664	1.834
32	0.985	0.985	1.030	0.768	0.770	1.294

Tables 3 to 4 present the percentage of rejection of the hypothesis $H_0 : \alpha = \beta = \gamma = 1$ for Lena and Baboon reference images. The results were obtained from 1,000 Monte Carlo simulations.

Table 3. Rejection percentages of H_0 for Lena image.

Number of looks	Filter: None	Lee	Enhanced Lee	Kuan
1	0.0	18.2	24.0	38.1
2	3.8	55.4	69.3	67.9
4	51.4	89.1	92.8	93.5
8	94.4	99.2	99.2	99.2
16	99.7	100.0	0.0	0.2
32	100.0	–	0.0	0.0

Table 4. Rejection percentages of H_0 for Baboon image.

Number of looks	Filter: None	Lee	Enhanced Lee	Kuan
1	3.9	31.9	33.9	40.4
2	27.4	61.2	68.3	70.6
4	67.8	87.8	88.5	91.9
8	94.3	94.1	95.1	98.5
16	99.6	94.2	86.4	94.1
32	100.0	12.1	8.2	53.8

Tables 5 and 6 present the averages of the SSIM index estimates under H_0 and H_1 for Lena and Baboon reference images. The results were obtained from 1,000 Monte Carlo simulations.

TABLE 5. Averages of the SSIM index estimates for Lena image.

Number of looks	No filter		Lee filter	
	Under H_0	Under H_1	Under H_0	Under H_1
1	0.413	0.413	0.704	0.629
2	0.549	0.548	0.801	0.781
4	0.682	0.662	0.871	0.823
8	0.795	0.729	0.920	0.856
16	0.879	0.799	0.953	0.891
32	0.933	0.848	0.973	0.933
Number of looks	Enhanced Lee filter		Kuan filter	
	Under H_0	Under H_1	Under H_0	Under H_1
1	0.724	0.718	0.792	0.782
2	0.860	0.835	0.881	0.859
4	0.929	0.890	0.931	0.893
8	0.962	0.913	0.959	0.908
16	0.979	0.979	0.975	0.975
32	0.987	0.987	0.985	0.985

TABLE 6. Averages of the SSIM index estimates for Baboon image.

Number of looks	No filter		Lee filter	
	Under H_0	Under H_1	Under H_0	Under H_1
1	0.258	0.258	0.496	0.480
2	0.383	0.372	0.624	0.580
4	0.527	0.476	0.732	0.645
8	0.670	0.545	0.817	0.712
16	0.790	0.611	0.878	0.798
32	0.876	0.698	0.919	0.871
Number of looks	Enhanced Lee filter		Kuan filter	
	Under H_0	Under H_1	Under H_0	Under H_1
1	0.509	0.492	0.560	0.539
2	0.672	0.620	0.689	0.636
4	0.780	0.692	0.784	0.678
8	0.847	0.737	0.850	0.712
16	0.886	0.812	0.896	0.821
32	0.909	0.907	0.929	0.910

Next, we display the Empirical CDF of the SSIM under H_0 (black) and H_1 (red) for several looks, based on 1,000 Monte Carlo simulations for images texmos2.S512, Lena and Baboon. (see Section 3 of the manuscript).

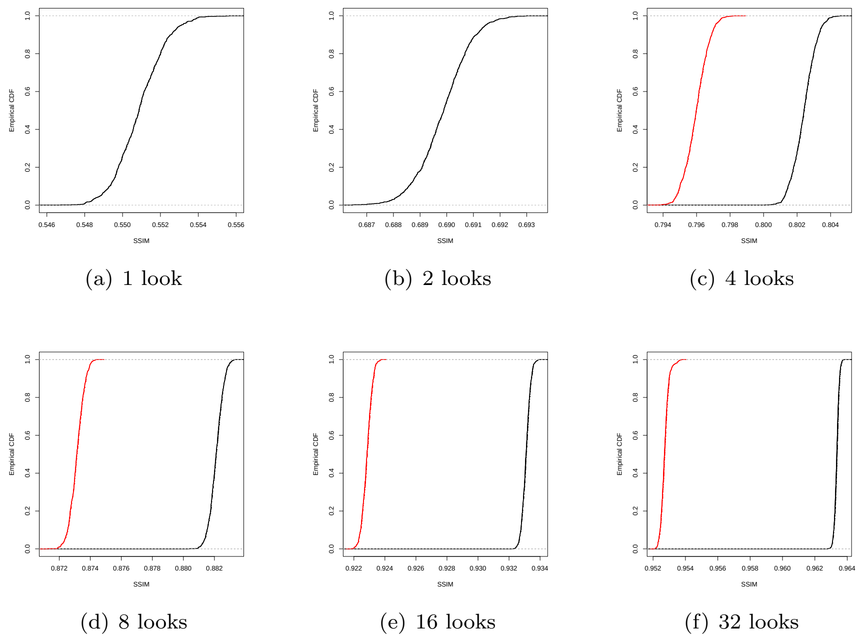

(a) 1 look (b) 2 looks (c) 4 looks

(d) 8 looks (e) 16 looks (f) 32 looks

FIGURE 1. Empirical CDFs: reference image texmos2.S512 using no filter.

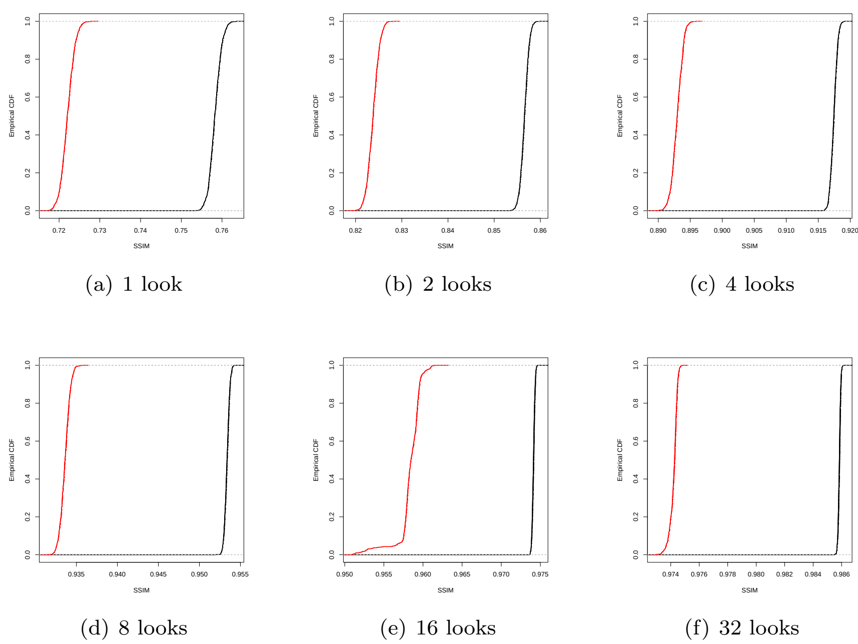

(a) 1 look (b) 2 looks (c) 4 looks

(d) 8 looks (e) 16 looks (f) 32 looks

FIGURE 2. Empirical CDFs: reference image texmos2.S512 using Lee filter.

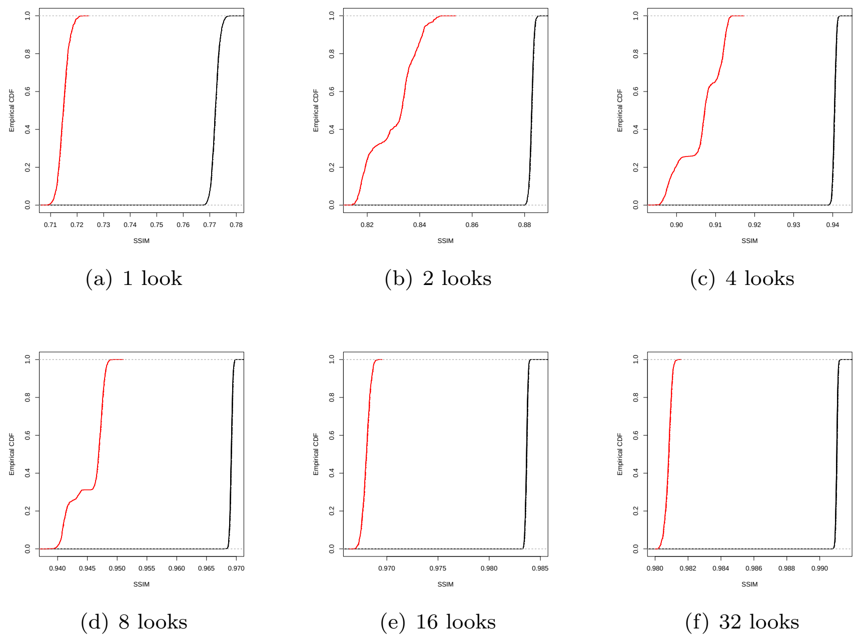

(a) 1 look (b) 2 looks (c) 4 looks

(d) 8 looks (e) 16 looks (f) 32 looks

FIGURE 3. Empirical CDFs: reference image texmos2.S512 using Enhanced Lee filter.

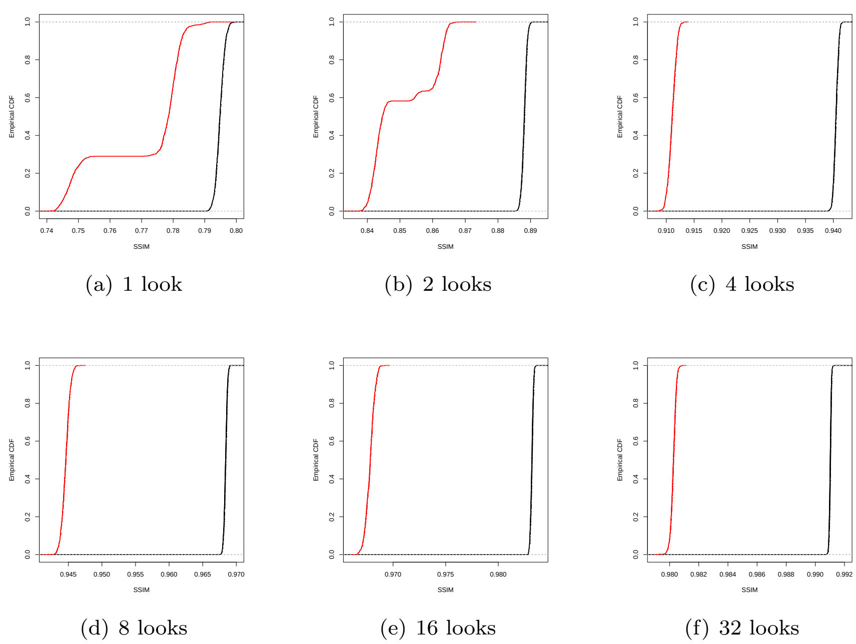

(a) 1 look (b) 2 looks (c) 4 looks

(d) 8 looks (e) 16 looks (f) 32 looks

FIGURE 4. Empirical CDFs: reference image texmos2.S512 using Kuan filter.

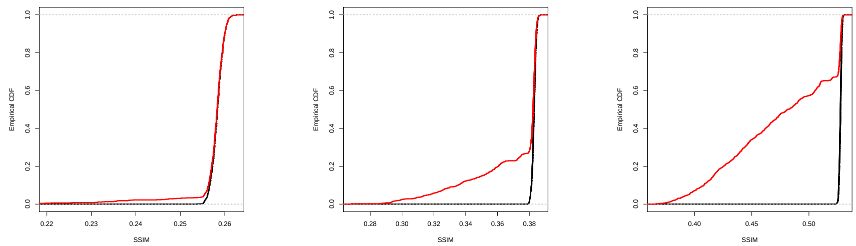

(a) 1 look (b) 2 looks (c) 4 looks

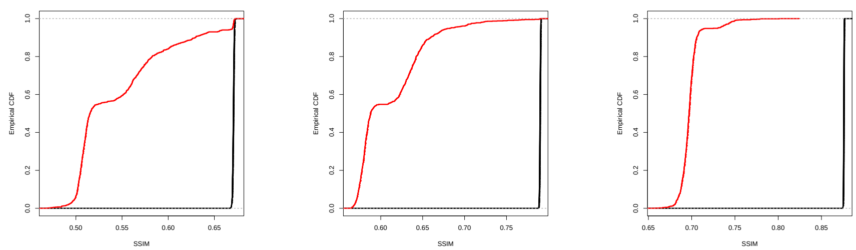

(d) 8 looks (e) 16 looks (f) 32 looks

FIGURE 5. Empirical CDFs: reference image Baboon using no filter.

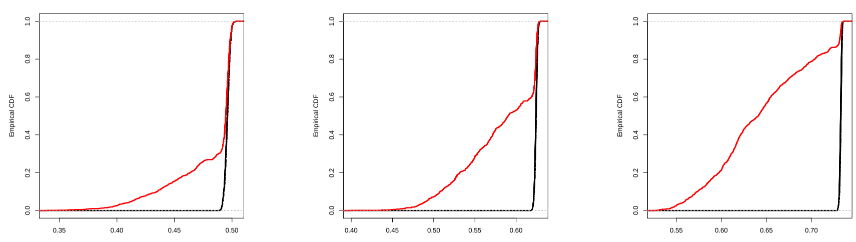

(a) 1 look (b) 2 looks (c) 4 looks

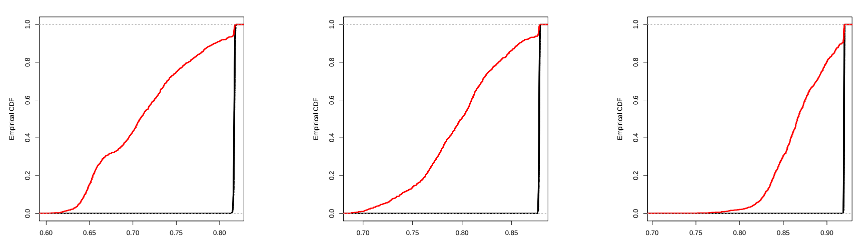

(d) 8 looks (e) 16 looks (f) 32 looks

FIGURE 6. Empirical CDFs: reference image Baboon using Lee filter.

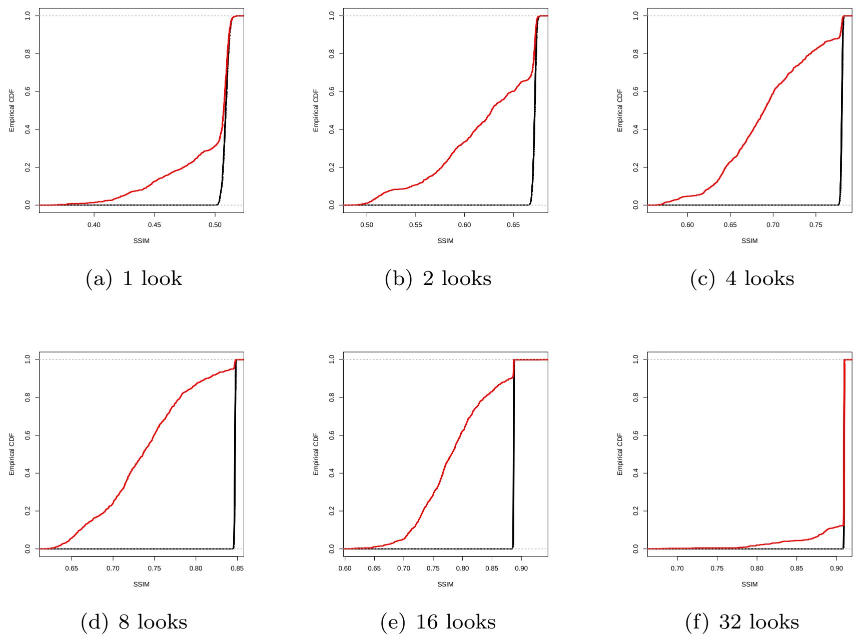

(a) 1 look (b) 2 looks (c) 4 looks

(d) 8 looks (e) 16 looks (f) 32 looks

FIGURE 7. Empirical CDFs: reference image Baboon using Enhanced Lee filter.

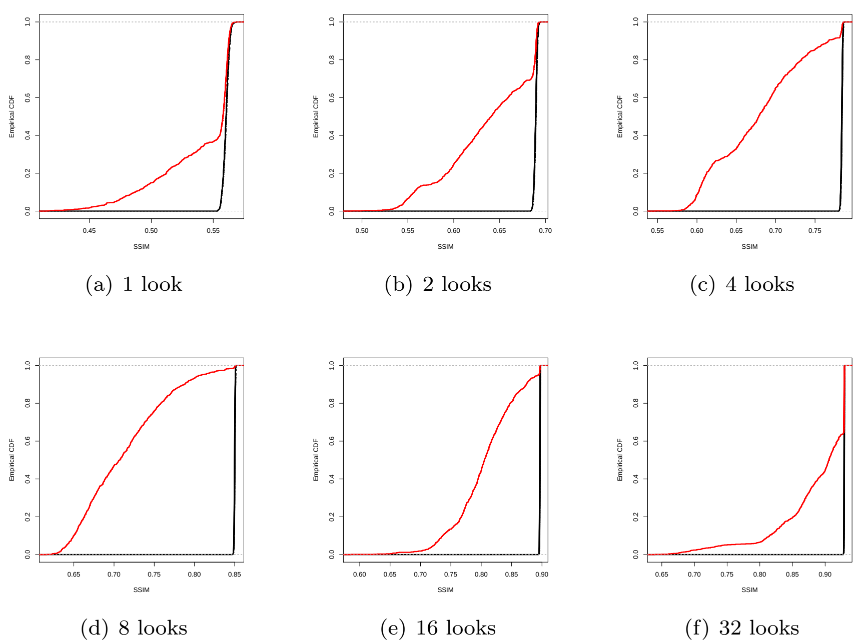

(a) 1 look (b) 2 looks (c) 4 looks

(d) 8 looks (e) 16 looks (f) 32 looks

FIGURE 8. Empirical CDFs: reference image Baboon using Kuan filter.

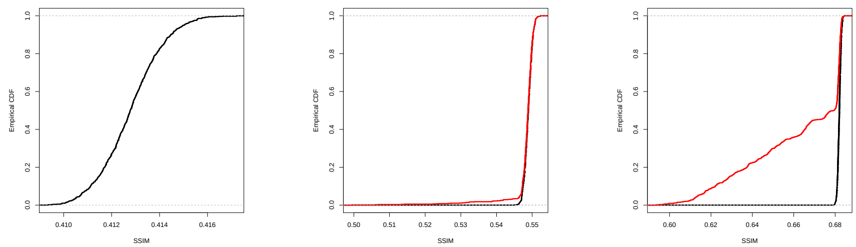

(a) 1 look (b) 2 looks (c) 4 looks

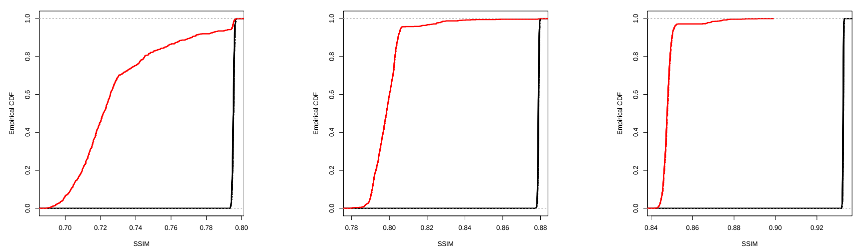

(d) 8 looks (e) 16 looks (f) 32 looks

FIGURE 9. Empirical CDFs: reference image Lena using no filter.

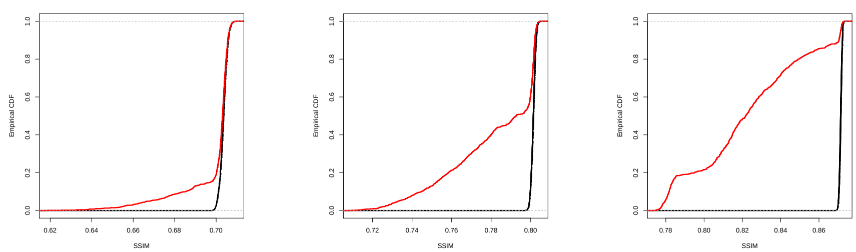

(a) 1 look (b) 2 looks (c) 4 looks

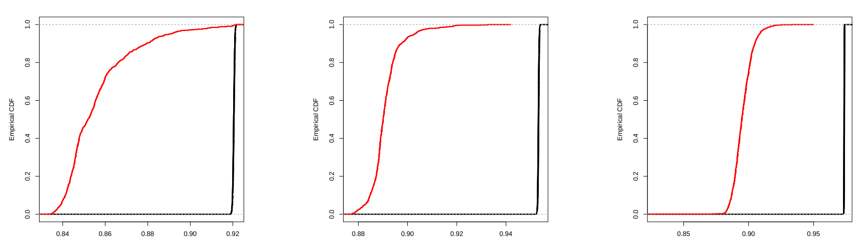

(d) 8 looks (e) 16 looks (f) 32 looks

FIGURE 10. Empirical CDFs: reference image Lena using Lee filter.

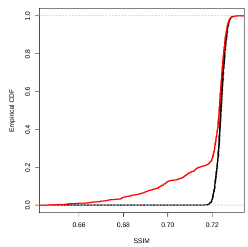

(a) 1 look

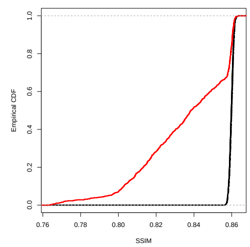

(b) 2 looks

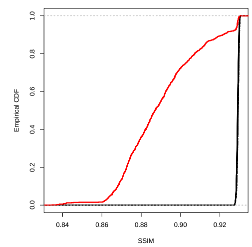

(c) 4 looks

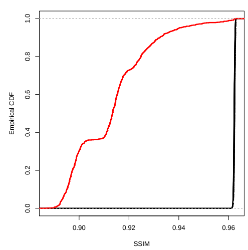

(d) 8 looks

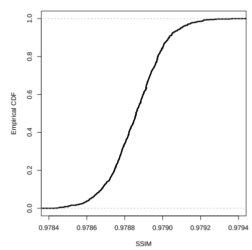

(e) 16 looks

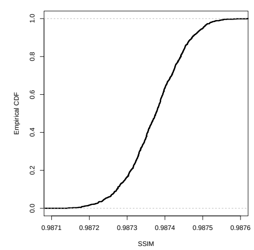

(f) 32 looks

FIGURE 11. Empirical CDFs: reference image `Lena` using Enhanced Lee filter.

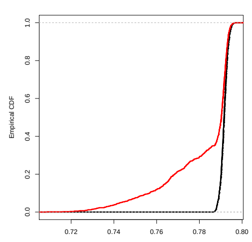

(a) 1 look

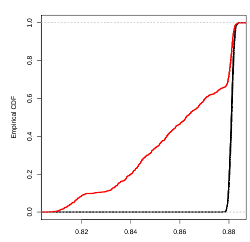

(b) 2 looks

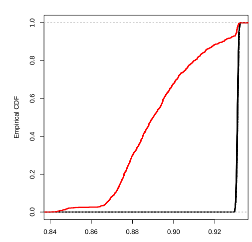

(c) 4 looks

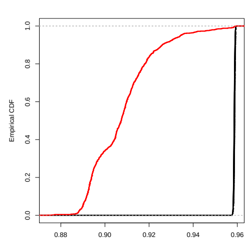

(d) 8 looks

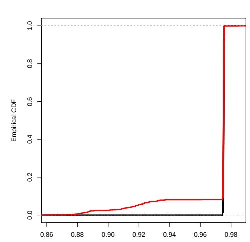

(e) 16 looks

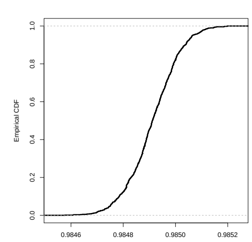

(f) 32 looks

FIGURE 12. Empirical CDFs: reference image `Lena` using Kuan filter.

Appendix B. Computation of score function for the nonlinear regression model with multiplicative noise

To reduce the computational effort associated with quasi-Newton algorithms (see, for instance Nash, 1990, Chap. 15) we can provide first-order information related to the nonlinear regression model defined by Equation (4) from the manuscript. Indeed, for the model with multiplicative noise, it follows that the log-likelihood function takes the form

$$\ell(\boldsymbol{\psi}) = -\frac{n}{2}\log 2\pi g^2(\phi) - \frac{1}{2}\log|\boldsymbol{W}(\boldsymbol{\theta})| - \frac{1}{2g^2(\phi)}(\boldsymbol{Z}-\phi\boldsymbol{f}(\boldsymbol{\theta}))^\top \boldsymbol{W}^{-1}(\boldsymbol{\theta})(\boldsymbol{Z}-\phi\boldsymbol{f}(\boldsymbol{\theta})),$$

with $\boldsymbol{f}(\boldsymbol{\theta}) = (f_1(\boldsymbol{\theta}),\dots,f_n(\boldsymbol{\theta}))^\top$ and $\boldsymbol{W}(\boldsymbol{\theta}) = \operatorname{diag}(f_1^2(\boldsymbol{\theta}),\dots,f_n^2(\boldsymbol{\theta}))$. Therefore, the first differential of $\ell(\boldsymbol{\psi})$ with respect to $\boldsymbol{\theta}$ is given by

$$\begin{aligned}\mathsf{d}_\theta\,\ell(\boldsymbol{\psi}) &= \frac{\phi}{g^2(\phi)}\big(\mathsf{d}_\theta\,\boldsymbol{f}(\boldsymbol{\theta})\big)^\top \boldsymbol{W}^{-1}(\boldsymbol{\theta})(\boldsymbol{Z}-\phi\boldsymbol{f}(\boldsymbol{\theta})) \\ &\quad - \frac{1}{2}\operatorname{tr}\boldsymbol{W}^{-1}(\boldsymbol{\theta})\Big\{\boldsymbol{W}(\boldsymbol{\theta}) - \frac{\boldsymbol{r}(\boldsymbol{\theta})\boldsymbol{r}^\top(\boldsymbol{\theta})}{g^2(\phi)}\Big\}\boldsymbol{W}^{-1}(\boldsymbol{\theta})\,\mathsf{d}_\theta\,\boldsymbol{W}(\boldsymbol{\theta}),\end{aligned} \tag{B.1}$$

where $\boldsymbol{r}(\boldsymbol{\theta}) = \boldsymbol{Z} - \phi\boldsymbol{f}(\boldsymbol{\theta})$. Using properties of the trace operator and applying the first identification theorem of Magnus and Neudecker (2007), we obtain that the score function $\boldsymbol{U}(\boldsymbol{\theta}) = \partial\ell(\boldsymbol{\psi})/\partial\boldsymbol{\theta}$ assumes the form:

$$\boldsymbol{U}(\boldsymbol{\theta}) = \boldsymbol{U}_1(\boldsymbol{\theta}) + \boldsymbol{U}_2(\boldsymbol{\theta}),$$

where

$$\begin{aligned}\boldsymbol{U}_1(\boldsymbol{\theta}) &= \frac{\phi}{g^2(\phi)}\boldsymbol{F}^\top(\boldsymbol{\theta})\boldsymbol{W}^{-1}(\boldsymbol{\theta})(\boldsymbol{Z}-\phi\boldsymbol{f}(\boldsymbol{\theta})), \\ \boldsymbol{U}_2(\boldsymbol{\theta}) &= -\frac{1}{2}\boldsymbol{H}^\top(\boldsymbol{\theta})\boldsymbol{V}^{-1}(\boldsymbol{\theta})\operatorname{vec}\Big(\boldsymbol{W}(\boldsymbol{\theta}) - \frac{\boldsymbol{r}(\boldsymbol{\theta})\boldsymbol{r}^\top(\boldsymbol{\theta})}{g^2(\phi)}\Big),\end{aligned}$$

with $\boldsymbol{H}(\boldsymbol{\theta}) = (\operatorname{vec}(\partial\boldsymbol{W}(\boldsymbol{\theta})/\partial\theta_1),\dots,\operatorname{vec}(\partial\boldsymbol{W}(\boldsymbol{\theta})/\partial\theta_p))$, p is the the dimension of $\boldsymbol{\theta}$, $\operatorname{vec}(\cdot)$ denotes the vectorization operator, $\boldsymbol{V}(\boldsymbol{\theta}) = \boldsymbol{W}(\boldsymbol{\theta})\otimes\boldsymbol{W}(\boldsymbol{\theta})$ and $\otimes$ indicates the Kronecker product.

Below we describe the computational strategy adopted in our C routines to evaluate the score function for the nonlinear regression model with multiplicative noise. Thus, we exploit the diagonal structure of $\boldsymbol{W}(\boldsymbol{\theta})$ to compute the elements of $\boldsymbol{U}_2(\boldsymbol{\theta})$ in a computationally efficient fashion. Noticing that

$$\frac{\partial\boldsymbol{W}(\boldsymbol{\theta})}{\partial\theta_j} = 2\operatorname{diag}(f_1(\boldsymbol{\theta})\dot{f}_{1j}(\boldsymbol{\theta}),\dots,f_n(\boldsymbol{\theta})\dot{f}_{nj}(\boldsymbol{\theta})),$$

where $\dot{f}_{ij}(\boldsymbol{\theta}) = \partial f_i(\boldsymbol{\theta})/\partial\theta_j$, for $i=1,\dots,n$; $j=1,\dots,p$, yields that the the jth element of $\boldsymbol{U}_2(\boldsymbol{\theta})$ takes the form

$$-\operatorname{tr}\boldsymbol{W}^{-1}(\boldsymbol{\theta})\boldsymbol{W}_j(\boldsymbol{\theta}) + \frac{1}{g^2(\phi)}\boldsymbol{r}^\top(\boldsymbol{\theta})\boldsymbol{W}^{-1}(\boldsymbol{\theta})\boldsymbol{W}_j(\boldsymbol{\theta})\boldsymbol{W}^{-1}(\boldsymbol{\theta})\boldsymbol{r}(\boldsymbol{\theta}), \tag{B.2}$$

for $j=1,\dots,p$, with $\boldsymbol{W}_j(\boldsymbol{\theta}) = \frac{1}{2}\partial\boldsymbol{W}(\boldsymbol{\theta})/\partial\theta_j$ and $\boldsymbol{r}(\boldsymbol{\theta}) = \boldsymbol{Z}-\phi\boldsymbol{f}(\boldsymbol{\theta})$. Simple calculations allow us to note that the first term of Equation (B.2) is given by

$$\operatorname{tr}\boldsymbol{W}^{-1}(\boldsymbol{\theta})\boldsymbol{W}_j(\boldsymbol{\theta}) = \sum_{i=1}^n \frac{\partial f_i(\boldsymbol{\theta})/\partial\theta_j}{f_i(\boldsymbol{\theta})}, \tag{B.3}$$

which is equivalent to adding all the elements of the jth column of the matrix $\boldsymbol{W}^{-1/2}(\boldsymbol{\theta})\boldsymbol{F}(\boldsymbol{\theta})$. Moreover, the second term of (B.2) assumes the form

$$\frac{1}{g^2(\phi)}\{\boldsymbol{W}^{-1}(\boldsymbol{\theta})\boldsymbol{r}(\boldsymbol{\theta})\}^\top \boldsymbol{W}_j(\boldsymbol{\theta})\boldsymbol{W}^{-1}(\boldsymbol{\theta})\boldsymbol{r}(\boldsymbol{\theta}) = \frac{1}{g^2(\phi)}\sum_{i=1}^{n}\Big(\frac{r_i(\boldsymbol{\theta})}{f_i^2(\boldsymbol{\theta})}\Big)^2\frac{\partial f_i(\boldsymbol{\theta})}{\partial\theta_j}. \quad \text{(B.4)}$$

Our implementation computes efficiently the score $\boldsymbol{U}(\boldsymbol{\theta})$ evaluating (B.3) and (B.4), as well as the cross product defined by $\boldsymbol{U}_1(\boldsymbol{\theta})$ by using the Fortran routine `dgemm` from the BLAS library (Lawson et al., 1979) included in the R software (R Core Team, 2020).

Appendix C. Expected information matrix for the nonlinear regression model with multiplicative noise

Here, we derive the differentials $\mathsf{d}^2_\psi\,\ell(\boldsymbol{\psi})$, $\boldsymbol{\psi} = (\boldsymbol{\theta}^\top, \phi)^\top$ for the heteroscedastic nonlinear regression model defined in Section 2 from the manuscript. The Fisher information matrix $\boldsymbol{\mathcal{F}}(\boldsymbol{\psi})$ is obtained efficiently using the differentiation method and by applying some identification theorems discussed in Magnus and Neudecker (2007).

Taking the differential of $\mathsf{d}_\theta\,\ell(\boldsymbol{\psi})$ given in (B.1) with respect to $\boldsymbol{\theta}$, we get

$$\begin{aligned}
\mathsf{d}^2_\theta\,\ell(\boldsymbol{\psi}) &= \frac{1}{2}\operatorname{tr}\boldsymbol{W}^{-1}(\boldsymbol{\theta})\,\mathsf{d}_\theta\,\boldsymbol{W}(\boldsymbol{\theta})\boldsymbol{W}^{-1}(\boldsymbol{\theta})\,\mathsf{d}_\theta\,\boldsymbol{W}(\boldsymbol{\theta}) \\
&\quad - \frac{1}{2}\operatorname{tr}\boldsymbol{W}^{-1}(\boldsymbol{\theta})\,\mathsf{d}^2_\theta\,\boldsymbol{W}(\boldsymbol{\theta}) - \frac{\phi^2}{g^2(\phi)}(\mathsf{d}_\theta\,\boldsymbol{f}(\boldsymbol{\theta}))^\top\boldsymbol{W}^{-1}(\boldsymbol{\theta})\,\mathsf{d}_\theta\,\boldsymbol{f}(\boldsymbol{\theta}) \\
&\quad - \frac{2\phi}{g^2(\phi)}(\mathsf{d}_\theta\,\boldsymbol{f}(\boldsymbol{\theta}))^\top\boldsymbol{W}^{-1}(\boldsymbol{\theta})\,\mathsf{d}_\theta\,\boldsymbol{W}(\boldsymbol{\theta})\boldsymbol{W}^{-1}(\boldsymbol{\theta})\boldsymbol{r}(\boldsymbol{\theta}) \\
&\quad + \frac{\phi}{g^2(\phi)}(\mathsf{d}^2_\theta\,\boldsymbol{f}(\boldsymbol{\theta}))^\top\boldsymbol{W}^{-1}(\boldsymbol{\theta})\boldsymbol{r}(\boldsymbol{\theta}) \\
&\quad + \frac{1}{2g^2(\phi)}\boldsymbol{r}^\top(\boldsymbol{\theta})\boldsymbol{W}^{-1}(\boldsymbol{\theta})\,\mathsf{d}^2_\theta\,\boldsymbol{W}(\boldsymbol{\theta})\boldsymbol{W}^{-1}(\boldsymbol{\theta})\boldsymbol{r}(\boldsymbol{\theta}) \\
&\quad - \frac{1}{g^2(\phi)}\boldsymbol{r}^\top(\boldsymbol{\theta})\boldsymbol{W}^{-1}(\boldsymbol{\theta})\,\mathsf{d}_\theta\,\boldsymbol{W}(\boldsymbol{\theta})\boldsymbol{W}^{-1}(\boldsymbol{\theta})\,\mathsf{d}_\theta\,\boldsymbol{W}(\boldsymbol{\theta})\boldsymbol{W}^{-1}(\boldsymbol{\theta})\boldsymbol{r}(\boldsymbol{\theta}).
\end{aligned}$$

Using that

$$\mathrm{E}\{\boldsymbol{r}(\boldsymbol{\theta})\} = \boldsymbol{0}, \quad \text{and} \quad \mathrm{E}\{\boldsymbol{r}(\boldsymbol{\theta})\boldsymbol{r}^\top(\boldsymbol{\theta})\} = g^2(\phi)\boldsymbol{W}(\boldsymbol{\theta}), \qquad \text{(B.1)}$$

yields that the negative of the expectation of the second differential of $\ell(\boldsymbol{\psi})$ with respect to $\boldsymbol{\theta}$ assumes the form

$$\begin{aligned}
\mathrm{E}\{-\,\mathsf{d}^2_\theta\,\ell(\boldsymbol{\psi})\} &= \frac{1}{2}\operatorname{tr}\boldsymbol{W}^{-1}(\boldsymbol{\theta})\,\mathsf{d}\,\boldsymbol{W}(\boldsymbol{\theta})\boldsymbol{W}^{-1}(\boldsymbol{\theta})\,\mathsf{d}_\theta\,\boldsymbol{W}(\boldsymbol{\theta}) \\
&\quad + \frac{\phi^2}{g^2(\phi)}(\mathsf{d}_\theta\,\boldsymbol{f}(\boldsymbol{\theta}))^\top\boldsymbol{W}^{-1}(\boldsymbol{\theta})\,\mathsf{d}_\theta\,\boldsymbol{f}(\boldsymbol{\theta}) \\
&= \frac{\phi^2}{g^2(\phi)}(\mathsf{d}_\theta\,\boldsymbol{f}(\boldsymbol{\theta}))^\top\boldsymbol{W}^{-1}(\boldsymbol{\theta})\,\mathsf{d}_\theta\,\boldsymbol{f}(\boldsymbol{\theta}) \\
&\quad + \frac{1}{2}(\mathsf{d}_\theta\operatorname{vec}\boldsymbol{W}(\boldsymbol{\theta}))^\top(\boldsymbol{W}^{-1}(\boldsymbol{\theta})\otimes\boldsymbol{W}^{-1}(\boldsymbol{\theta}))\,\mathsf{d}_\theta\operatorname{vec}\boldsymbol{W}(\boldsymbol{\theta}). \qquad \text{(B.2)}
\end{aligned}$$

Taking the first and second differential of $\ell(\boldsymbol{\psi})$ with respect to ϕ we have

$$\begin{aligned}
\mathsf{d}_\phi\,\ell(\boldsymbol{\psi}) &= -\frac{n}{2}\frac{\mathsf{d}\,g^2(\phi)}{2g^2(\phi)} + \frac{\boldsymbol{f}^\top(\boldsymbol{\theta})\boldsymbol{W}^{-1}(\boldsymbol{\theta})\boldsymbol{r}(\boldsymbol{\theta})\,\mathsf{d}\,\phi}{g^2(\phi)} + \frac{\boldsymbol{r}^\top(\boldsymbol{\theta})\boldsymbol{W}^{-1}(\boldsymbol{\theta})\boldsymbol{r}(\boldsymbol{\theta})\,\mathsf{d}\,g^2(\phi)}{2g^4(\phi)} \\
\mathsf{d}^2_\phi\,\ell(\boldsymbol{\psi}) &= -\frac{n}{2}\Big[\frac{g^2(\phi)\,\mathsf{d}^2\,g^2(\phi) - \mathsf{d}\,g^2(\phi)\,\mathsf{d}\,g^2(\phi)}{g^4(\phi)}\Big] - \frac{\boldsymbol{f}^\top(\boldsymbol{\theta})\boldsymbol{W}^{-1}(\boldsymbol{\theta})\boldsymbol{f}(\boldsymbol{\theta})\,\mathsf{d}\,\phi\,\mathsf{d}\,\phi}{g^2(\phi)} \\
&\quad - \frac{2\boldsymbol{f}^\top(\boldsymbol{\theta})\boldsymbol{W}^{-1}(\boldsymbol{\theta})\boldsymbol{r}(\boldsymbol{\theta})\,\mathsf{d}\,\phi\,\mathsf{d}\,g^2(\phi)}{g^4(\phi)} + \frac{\boldsymbol{r}^\top(\boldsymbol{\theta})\boldsymbol{W}^{-1}(\boldsymbol{\theta})\boldsymbol{r}(\boldsymbol{\theta})\,\mathsf{d}^2\,g^2(\phi)}{2g^4(\phi)} \\
&\quad - \frac{\boldsymbol{r}^\top(\boldsymbol{\theta})\boldsymbol{W}^{-1}(\boldsymbol{\theta})\boldsymbol{r}(\boldsymbol{\theta})\,\mathsf{d}\,g^2(\phi)\,\mathsf{d}\,g^4(\phi)}{g^8(\phi)}.
\end{aligned}$$

Notice that

$$\mathsf{d}\,g^2(\phi) = 2\phi(2\phi^2 - 1)\,\mathsf{d}\,\phi, \qquad \mathsf{d}\,g^4(\phi) = 4\phi^3(2\phi^4 - 3\phi^2 - 1)\,\mathsf{d}\,\phi. \tag{B.3}$$

Then the first differential of $\ell(\boldsymbol{\psi})$ with respect to ϕ can be written as:

$$\mathsf{d}_\phi\,\ell(\boldsymbol{\psi}) = \frac{\boldsymbol{f}^\top(\boldsymbol{\theta})\boldsymbol{W}^1(\boldsymbol{\theta})\boldsymbol{r}(\boldsymbol{\theta})}{g^2(\phi)}\,\mathsf{d}\,\phi - \frac{2\phi^2 - 1}{\phi^3(\phi^2 - 1)}\big[n\phi^2 - \boldsymbol{r}^\top(\boldsymbol{\theta})\boldsymbol{W}^{-1}(\boldsymbol{\theta})\boldsymbol{r}(\boldsymbol{\theta})\big]\,\mathsf{d}\,\phi.$$

From (B.1) and (B.3) and using simple algebra, we obtain

$$\begin{aligned}
\mathrm{E}\{-\,\mathsf{d}^2_\phi\,\ell(\boldsymbol{\psi})\} &= \frac{1}{g^2(\phi)}\Big[\boldsymbol{f}^\top(\boldsymbol{\theta})\boldsymbol{W}^{-1}(\boldsymbol{\theta})\boldsymbol{f}(\boldsymbol{\theta})\,\mathsf{d}\,\phi\,\mathsf{d}\,\phi - \frac{n}{2}\frac{\mathsf{d}\,g^2(\phi)}{g^2(\phi)}\Big\{\mathsf{d}\,g^2(\phi) - \frac{\mathsf{d}\,g^4(\phi)}{g^2(\phi)}\Big\}\Big] \\
&= \frac{1}{g^2(\phi)}\Big[\boldsymbol{f}^\top(\boldsymbol{\theta})\boldsymbol{W}^{-1}(\boldsymbol{\theta})\boldsymbol{f}(\boldsymbol{\theta}) + \frac{2nq(\phi)}{(\phi^2 - 1)^2}\Big]\,\mathsf{d}\,\phi\,\mathsf{d}\,\phi,
\end{aligned} \tag{B.4}$$

with $q(\phi) = (2\phi^2 - 1)(2\phi^4 - 3\phi^2 + 1)$. Differentiating $\mathsf{d}_\phi\,\ell(\boldsymbol{\psi})$ with respect to $\boldsymbol{\theta}$ we have

$$\begin{aligned}
\mathsf{d}^2_{\theta\phi}\,\ell(\boldsymbol{\psi}) &= \frac{\boldsymbol{r}^\top(\boldsymbol{\theta})\boldsymbol{W}^{-1}(\boldsymbol{\theta})\,\mathsf{d}_\theta\,\boldsymbol{f}(\boldsymbol{\theta})\,\mathsf{d}\,\phi}{g^2(\phi)} - \frac{\phi\boldsymbol{f}^\top(\boldsymbol{\theta})\boldsymbol{W}^{-1}(\boldsymbol{\theta})\,\mathsf{d}_\theta\,\boldsymbol{f}(\boldsymbol{\theta})\,\mathsf{d}\,\phi}{g^2(\phi)} \\
&\quad - \frac{\boldsymbol{f}^\top(\boldsymbol{\theta})\boldsymbol{W}^{-1}(\boldsymbol{\theta})\,\mathsf{d}_\theta\,\boldsymbol{W}(\boldsymbol{\theta})\boldsymbol{W}^{-1}(\boldsymbol{\theta})\boldsymbol{r}(\boldsymbol{\theta})\,\mathsf{d}\,\phi}{g^2(\phi)} - \frac{\phi\,\boldsymbol{r}^\top(\boldsymbol{\theta})\boldsymbol{W}^{-1}(\boldsymbol{\theta})\,\mathsf{d}_\theta\,\boldsymbol{f}(\boldsymbol{\theta})\,\mathsf{d}\,g^2(\phi)}{g^4(\phi)} \\
&\quad - \frac{\boldsymbol{r}^\top(\boldsymbol{\theta})\boldsymbol{W}^{-1}(\boldsymbol{\theta})\,\mathsf{d}_\theta\,\boldsymbol{W}(\boldsymbol{\theta})\boldsymbol{W}^{-1}(\boldsymbol{\theta})\boldsymbol{r}(\boldsymbol{\theta})\,\mathsf{d}\,g^2(\phi)}{2g^4(\phi)}
\end{aligned}$$

Taking expectations and using Equation (B.1), we obtain

$$\mathrm{E}\{-\,\mathsf{d}^2_{\theta\phi}\,\ell(\boldsymbol{\psi})\} = \frac{\phi}{g^2(\phi)}\big[\boldsymbol{f}^\top(\boldsymbol{\theta})\boldsymbol{W}^{-1}(\boldsymbol{\theta})\,\mathsf{d}_\theta\,\boldsymbol{f}(\boldsymbol{\theta}) + (2\phi^2 - 1)\operatorname{tr}\boldsymbol{W}^{-1}(\boldsymbol{\theta})\,\mathsf{d}_\theta\,\boldsymbol{W}(\boldsymbol{\theta})\big]\,\mathsf{d}\,\phi. \tag{B.5}$$

Thus, applying the second identification theorem of Magnus and Neudecker (2007) to $\mathrm{E}\{-\,\mathsf{d}^2_\theta\,\ell(\boldsymbol{\psi})\}$, $\mathrm{E}\{-\,\mathsf{d}^2_\phi\,\ell(\boldsymbol{\psi})\}$ and $\mathrm{E}\{-\,\mathsf{d}^2_{\theta\phi}\,\ell(\boldsymbol{\psi})\}$, given in Equations (B.2), (B.4) and (B.5), respectively leads to the Fisher information matrix,

$$\boldsymbol{\mathcal{F}}(\boldsymbol{\psi}) = \begin{pmatrix} \boldsymbol{\mathcal{F}}_{\theta\theta}(\boldsymbol{\psi}) & \boldsymbol{\mathcal{F}}_{\theta\phi}(\boldsymbol{\psi}) \\ \boldsymbol{\mathcal{F}}^\top_{\theta\phi}(\boldsymbol{\psi}) & \mathcal{F}_{\phi\phi}(\boldsymbol{\psi}) \end{pmatrix}, \tag{B.6}$$

where

$$\mathcal{F}_{\theta\theta}(\psi) = \frac{\phi^2}{g^2(\phi)} \boldsymbol{F}^\top(\boldsymbol{\theta})\boldsymbol{W}^{-1}(\boldsymbol{\theta})\boldsymbol{F}(\boldsymbol{\theta}) + \frac{1}{2}\boldsymbol{H}^\top(\boldsymbol{\theta})\boldsymbol{V}^{-1}(\boldsymbol{\theta})\boldsymbol{H}(\boldsymbol{\theta}),$$

$$\mathcal{F}_{\theta\phi}(\psi) = \frac{\phi}{g^2(\phi)}\Big\{\boldsymbol{F}^\top(\boldsymbol{\theta})\boldsymbol{W}^{-1}(\boldsymbol{\theta})\boldsymbol{f}(\boldsymbol{\theta}) + (2\phi^2-1)\boldsymbol{H}^\top(\boldsymbol{\theta}) \operatorname{vec} \boldsymbol{W}^{-1}(\boldsymbol{\theta})\Big\},$$

$$\mathcal{F}_{\phi\phi}(\psi) = \frac{1}{g^2(\phi)}\Big\{\boldsymbol{f}^\top(\boldsymbol{\theta})\boldsymbol{W}^{-1}(\boldsymbol{\theta})\boldsymbol{f}(\boldsymbol{\theta}) + \frac{2nq(\phi)}{(\phi^2-1)^2}\Big\},$$

with $\boldsymbol{H}(\boldsymbol{\theta}) \in \mathbb{R}^{n^2\times p}$ and $\boldsymbol{V}(\boldsymbol{\theta}) \in \mathbb{R}^{n^2\times n^2}$ defined in Equation (8) from the manuscript. Note that $\boldsymbol{\mathcal{F}}(\boldsymbol{\psi})$ can also be obtained in the way in which the results presented by Patriota et al. (2010) were obtained.

Appendix D. Removing multiplicative noise from an image

In order to describe the value of an image for a particular pixel, we denote an images as X such that the intensity at the location (i, j) is $X(i, j)$. Asume that the image X has been corrupted by a stationary multiplicative noise Y such that $Z = X \cdot Y$. Without loss of generality, we also assume that $\mathrm{E}(Y) = 1$. In practice, this is $\overline{Y} = 1$. Several filters for the multiplicative noise model has been proposed. For instance, Lee (1980) filter is derived from the equation

$$Z = X + (Y-1)X.$$

Under the unit-mean noise assumption, the pixel value estimate $\widehat{Z}(i, j)$ for Lee filter adopts the form:

$$\widehat{Z}(i,j) = \overline{Y} + K(Y_0 - \overline{Y}), \tag{D.1}$$

where the weight function, K is given by

$$K = \frac{S_Y^2}{S_Y^2 + \overline{Y}^2/L},$$

with $\overline{Y}$ and S_Y^2 are estimated from a local window, Y_0 represents the value at the center of the window, and L is the number of looks.

Another filter for multiplicative noise was developed by Kuan et al. (1987), which, such as Lee's filter, corresponds to a filter with minimum mean square error and is defined by (D.1), with weight function

$$K = \frac{\Delta^2}{\Delta^2 + (\overline{Y}^2 + \Delta^2)/L}, \qquad \Delta^2 = \frac{LS_Y^2 - \overline{Y}^2}{L+1}.$$

The last filter we will use in our experiments to remove multiplicative noise was developed by Lopes et al. (1990) as an enhancement of Lee's filter, and is defined as

$$\widehat{Z}(i,j) = \begin{cases} \overline{Y}, & CV \le 1/\sqrt{L}, \\ \overline{Y}K + Y_0(1-K), & 1/\sqrt{L} < CV < \sqrt{1+2/L}, \\ Y_0, & CV \ge \sqrt{1+2/L}, \end{cases}$$

where $CV = S_Y/\overline{Y}$ is the coefficient of variation of the local window, and

$$K = \exp\{-D(CV - 1/\sqrt{L})/(\sqrt{1+2/L} - CV)\},$$

with D being a damping factor.

References

Kuan, D.T., Sawchuk, A.A., Strand, T.C., Chavel, P. (1987). Adaptive restoration of images with speckle. *IEEE Transactions on Acoustics Speech and Signal Processing* **ASSP-35**, 373-383.

Lawson, C.L., Hanson, R.J., Kincaid, D., Krogh, F.T. (1979). Basic linear algebra subprograms for FORTRAN usage. *ACM Transactions on Mathematical Software* **5**, 308-323.

Lee, J.S. (1980). Digital image enhancement and noise filtering by use of local statistics. *IEEE Transactions on Pattern Analysis and Machine Intelligence* **PAMI-2**, 165-168.

Lopes, A., Touzi, R., Nezry, R. (1990). Adaptive speckle filters and scene heterogeneity. *IEEE Transactions on Geoscience and Remote Sensing* **28**, 992-1000.

Magnus, J.R., Neudecker, H. (2007). *Matrix Differential Calculus with Applications in Statistics and Econometrics*. Wiley, Chichester.

Nash, J.C. *Compact Numerical Methods for Computers. Linear Algebra and Function Minimization*. Bristol: Adam Hilger, 1990.

Patriota, A.G., Lemonte, A.J., de Castro, M. (2010). Influence diagnostics in a multivariate normal regression model with general parameterization. *Statistical Methodology* **7**, 644-654.

R Core Team (2020). *R: A Language and Environment for Statistical Computing*. R Foundation for Statistical Computing, Vienna, Austria. http://www.R-project.org

Departamento de Matemática, Universidad Técnica Federico Santa María

Current address: Departamento de Matemática, Universidad Técnica Federico Santa María, Av. España 1680, Casilla 110-V, Valparaíso, Chile

Orcid ID: orcid.org/0000-0002-4675-5201; orcid.org/0000-0001-5519-0946

Email address: felipe.osorios@usm.cl; ronny.vallejos@usm.cl

U-Planner, Chile

Current address: U-Planner, Avenida Tupungato 3850, Curauma, Valparaíso, Chile

Orcid ID: orcid.org/0000-0001-7377-3627

Email address: wilson.barraza@u-planner.com

Facultad de Matemática, Astronomía, Física y Computación, Universidad Nacional de Córdoba

Current address: Facultad de Matemática, Astronomía, Física y Computación, Universidad Nacional de Córdoba. Medina Allende s/n. Ciudad Universitaria (X5000HUA), Córdoba, Argentina.

Orcid ID: orcid.org/0000-0003-2870-7502

Email address: sm.ojeda@unc.edu.ar

Instituto de Diversidad y Ecología Animal, CONICET y Facultad de Ciencias Exactas Físicas y Naturales, Universidad Nacional de Córdoba

Current address: Instituto de Diversidad y Ecología Animal, CONICET y Facultad de Ciencias Exactas Físicas y Naturales, Universidad Nacional de Córdoba. Córdoba 5016, Argentina.

Orcid ID: orcid.org/0000-0001-7556-0748

Email address: marcoslandi1980@gmail.com